

Edge emission of ZnO grown on Si whiskers

CHARUS M. BRISKINA^{a,*}, VALERY M. MARKUSHEV^a, LUDMILA A. ZADOROZHNYAYA^b,
MIKHAIL E. GIVARGIZOV^b, VLADIMIR M. KANEVSKY^b

^a*Kotelnikov Institute of Radio-Engineering and Electronics of Russian Academy of Sciences, Mokhovaya 11-7, Moscow, 125009, Russian Federation*

^b*Shubnikov Institute of Crystallography of Federal Scientific Research Centre "Crystallography and Photonics" of Russian Academy of Sciences, Leninskiy Prospekt 59, Moscow, 119333, Russia*

ZnO nanostructures were grown on Si substrates by vapor-liquid-solid method and their edge luminescence and lasing were observed and analyzed. Two types of Si substrates were used: a substrate with Si whiskers and a substrate with Si whiskers covered with Au globules. It was found out that decomposition of luminescence spectra of the samples into Gaussian components allows assuming that spectra consist of three bands. Detailed analysis of the dependence of spectral position of all components on pump level showed that the first (high frequency) component is due to exciton recombination, the second one is a P line and the third one can be due to radiation related to defect level. Most likely this defect is interstitial zinc. In the case of the sample with Au on whiskers, lasing was observed from some regions of the sample where microcrystals served as optical resonators. Moreover, the use of Au noticeably increases intensity of P line and radiation due to defect level.

(Received September 29, 2020; accepted April 8, 2021)

Keywords: ZnO, Whiskers, Luminescence, Lasing, Si Substrate, Au Globules, P line

1. Introduction

Zinc oxide is wide band-gap semiconductor with the band-gap width $E_g \approx 3.3$ eV at room temperature and exciton binding energy 60 meV. Due to these characteristics it is possible to register ZnO edge emission at room and higher temperature, for example [1].

ZnO interesting peculiarity is great diversity of structures of different morphology. Such variation provided by sometimes only a little different growth conditions. Together with the use of different methods and phenomena influencing the physical properties of ZnO, it leads to variants of luminescence spectra and their behavior under varying excitation conditions. Attracting optical properties and their modifications were reported for such 1D structures like ZnO nanorods, whiskers, and tetrapods [2-9], for 2D structures like ZnO nanosheets, nanoplates, nanowalls, and thin films [17-22], and bulk structures like ZnO microrods and thick films 0-0. In proposed paper edge emission spectra of ZnO nanostructures grown on Si substrates with whiskers were analyzed. The peculiarities of luminescence and lasing of these nanostructures were studied. Variants with Au and without it are considered.

Spectra obtained are wide bands with complex contours. This indicates the presence in the spectra of

some components with different nature. On this basis spectra analysis was performed by their decomposition into components. As a result of analysis it was shown that the type of these components dependence on pumping level allows concluding that in spectra free exciton recombination emission, P line and defect level emission are present. Most likely the defect is interstitial zinc.

2. Experimental

ZnO was grown on (111) Si substrates by the gas-transport method from Zn vapor and O₂ using the vapor-liquid-crystal (VLC) mechanism [23]. Si whiskers were preliminary formed using the technique described in [24]. For synthesis of samples with Au, the Au layer (~100 nm) was preliminary deposited on the substrate. This technique allows to preserve Au globules on the tops of the whiskers. The shape of globule is near to hemisphere with radius of ~100 nm.

Fig. 1 shows SEM image and element mapping images of Si substrate with whiskers covered with Au globules. In can be seen that Au presents only on the top of the whiskers.

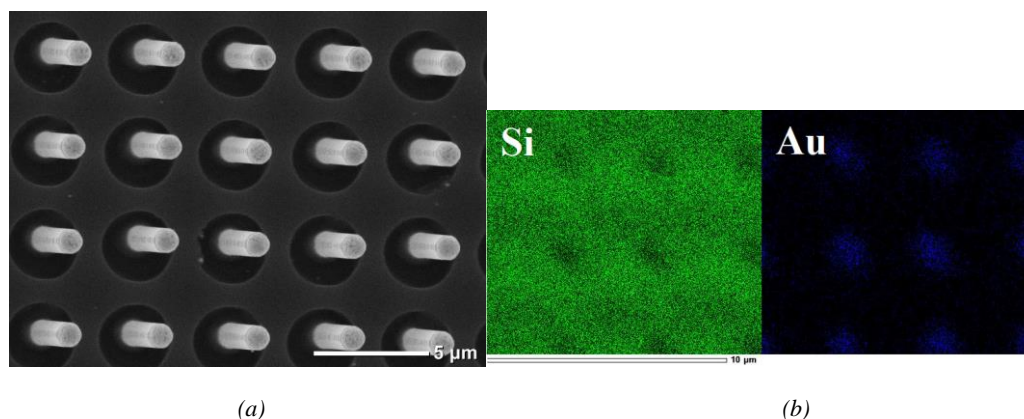


Fig. 1. SEM image (a) and element mapping images (b) of Si substrate with whiskers covered with Au globules (color online)

Fig. 2 demonstrates SEM images of ZnO grown on Si whiskers without Au (sample No.1) and ZnO grown on Si whiskers with Au globules (sample No. 2).

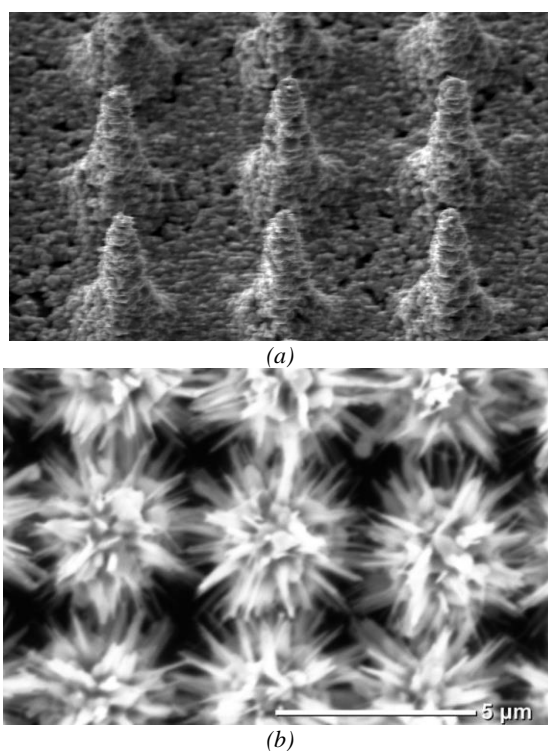


Fig. 2. SEM images of structures analyzed: a) sample No.1 (ZnO on whiskers without Au); b) sample No.2 (ZnO on whiskers with Au globules). The distribution of the whiskers in both samples is the same.

Au forms a low-melting eutectic with Zn. As a result during ZnO crystallization (550-580°C), the globule is solution of silicon in an Au melt. Such VLC process is catalytic, i.e. insignificant consumption of metal-solvent (Au) for alloying the growing crystal can be ignored. A typical picture of discrete systems of disoriented ZnO micro crystallites on the “pedestal” of Si whiskers is shown in Fig. 2b. The energy dispersive X-ray (EDX) analysis of this sample (Fig. 3) finds 0.4 at.% of Au besides Zn, O, and Si on the top of the whiskers, which corroborates the VLS mechanism of ZnO growth.

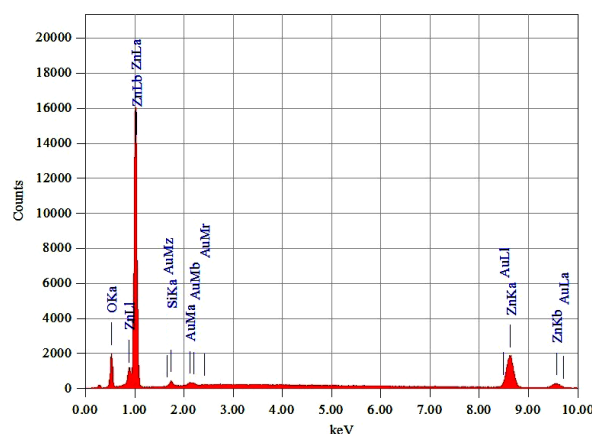


Fig. 3. EDX result for sample No. 2 (color online)

A completely different morphological picture was observed when growing ZnO micro crystallites on Si whiskers from the tops of which Au globules were removed by chemical etching. In this case, Zn is both a catalyst and a precursor for the synthesis of ZnO. Oxygen molecules diffuse through Zn vapor to the substrate, where they are adsorbed by Zn droplets and react with it to form oxide. As the number of ZnO nuclei increases, the substrate surface overgrows rapidly with a polycrystalline film (Fig. 2a).

Photoexcitation of samples was made with the 3rd harmonics of pulsed Nd:YAG laser (355 nm) with pulse duration of 10 ns and repetition rate of 15 Hz. The energy of pumping pulses was varied by a polarizing filter and measured with Ophir Photonics PD10-C. The pumping spot size on a sample was ~180 μm. The registration of samples emission was carried out by using monochromator MDR-206 with the CCD camera on its exit slit. Depending on the level of the signal, accumulation of pulses (from 50 up to 400) was used.

3. Results and discussion

Further, the results of spectra analyzing for samples No. 1 and No. 2 are presented.

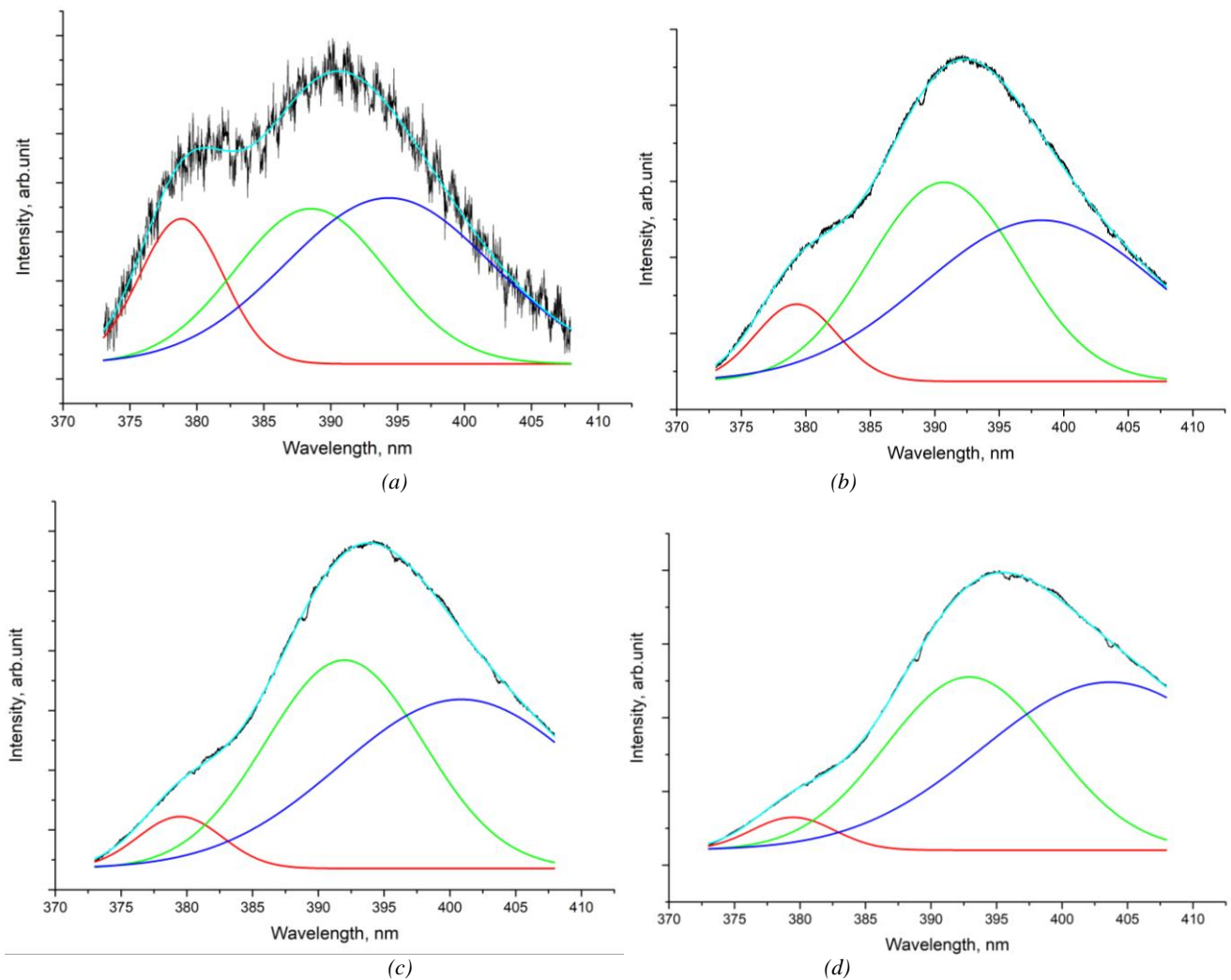


Fig. 4. PL spectra of the sample No.1 decomposed into 3 components recorded under pumping energy of a) 0.09 μJ ; b) 0.57 μJ ; c) 1.26 μJ ; d) 2.97 μJ (color online)

In Fig. 4 examples of photoluminescence (PL) spectra of the sample No.1 obtained at the pumping pulse energy from 0.09 μJ up to 2.97 μJ are shown. All spectra are decomposed into three Gaussian components which provides best fitting of the spectra (under relatively low pumping energy two-components fitting is also allowable).

It is clearly seen from the PL spectra that with an increase in the pump level, the intensity of the 1st component relative to the intensities of the 2nd and 3rd components decreases markedly. This, most likely, is the result of an increase in the number of inelastic collisions of excitons with pumping, leading to the appearance of a P-line and, accordingly, to a decrease in the number of excitons that did not experience collisions. The dependence on the pump of the integrated intensities of all three components of the spectrum will be considered below.

Since the exciton binding energy is 0.06 eV, using the position of the 1st component maximum at low pumping (3.273 eV) it is possible to estimate approximately the band-gap in sample No.1 at room temperature as ~ 3.33 eV.

It can be seen from the spectra that the exciton recombination emission energy decreases slightly from 3.273 eV to 3.269 eV with increasing pump up to 0.57 μJ , and with a further increase in pumping up to 2.97 μJ , it practically does not change, although the sample is undoubtedly heated. This should lead to a decrease in the band-gap and, accordingly, to a decrease in the energy of photons emitted as a result of spontaneous recombination of excitons. It can be assumed that the narrowing of the forbidden band is compensated by the effect of partial filling of the conduction band with electrons (Burshtein-Moss effect). Below, the possibility of the existence of this effect under the conditions of the experiment will be discussed in detail.

Let us analyze the origin of the 2nd component. Fig. 5 shows the dependences on pumping of energy shifts of the 2nd and the 3rd components relatively to the 1st one.

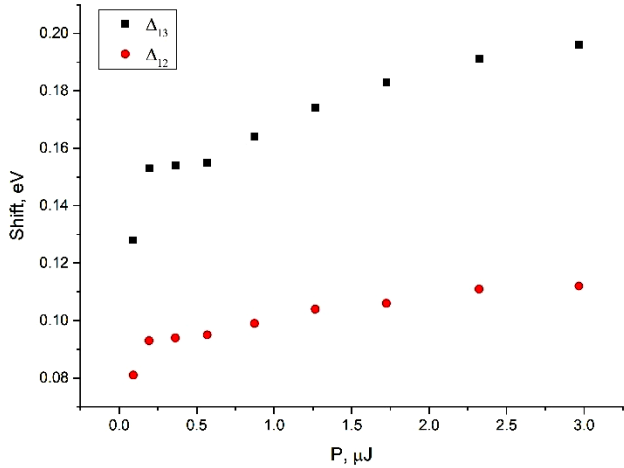


Fig. 5. Dependence on the pumping of energy shifts of the 2nd and 3rd components relative to the 1st one (color online)

Basing on spectral shift of the 2nd component relative to the 1st one it can be assumed that this band is due to scattering of the exciton either on the exciton (ex-ex) or on the electron (ex-el) [25]. In the case of ex-ex, the energy of the resulting photon is less than the energy of the maximum of the spontaneous recombination band of the exciton, by

$$\Delta_{12} = E_b \left(1 - \frac{1}{n^2}\right) + \frac{3}{2}kT \quad (1)$$

where E_b is the exciton binding energy, the n is number of the level at which the exciton is excited by inelastic collision, $\frac{3}{2}kT$ is the kinetic additive due to the thermal motion of the exciton. In the second variant (ex-el), the value of Δ_{12} is γkT [25]. At the transition point from the first variant to the second, the value Δ_{12} at $n = \infty$, i.e. $60 + \frac{3}{2}kT = \gamma kT$. Suppose that in the spectra considered by us, the 2nd component is due to ex-el scattering. With minimal pumping, we can consider that temperature is 300K ($kT = 26$ meV), then $82 = \gamma kT$ and $\gamma = 3.17$. This means that the transition from ex-ex to ex-el should be at $kT = 60/(\gamma - 3/2) = 36$ eV, which corresponds to a temperature of 417 K, i.e. the assumption is wrong.

Thus, most likely the second component is a P line. Using the experimental data for Δ_{12} and Eq. (1), we can try to estimate the dependence on the pump of the temperature range of the sample. For this, two variants of calculating the dependence of temperature on pumping were performed: i) choosing the values of n that give the minimum temperature T_1 ; ii) considering $n = 2$ in Eq. (1) – this is the case when the temperature T_1 is the maximum possible temperature.

In Fig. 6, T_1 defines the lower boundary of the possible interval; T_2 defines its upper boundary.

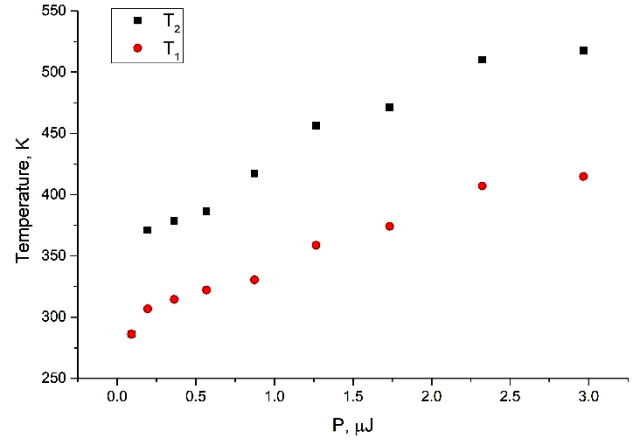


Fig. 6. Dependence on the pumping of the possible temperature range of the sample during its pumping (color online)

The following values of the final temperature were obtained (at pumping of 2.97 μ J): the upper boundary $T_2 = 518$ K, i.e. the maximum possible heating is 218^oC, the lower limit is $T_1 = 415$ K, i.e. the minimum possible heating is 115^oC. According to [26], a narrowing of the band-gap at a ZnO temperature above 200 K is 0.35 meV/K. Accordingly, in the experiment under consideration, the upper limit of the band gap narrowing is 76 meV, the lower limit is 40 meV, the average value is 58 meV. It should be noted that these results should be considered a rather rough estimation.

Assuming that partial filling of the conduction band with electrons compensates the narrowing of the band-gap, we estimate the electron concentration needed for compensation of 58 meV using equation:

$$N(E) = \frac{8\pi}{3} \left(\frac{2m_e}{h^2}\right)^{3/2} (E_c - E)^{3/2} \quad (2)$$

true for the energies near the band minimum. In (2), m_e is the effective electron mass, E_c is a conduction band minimum energy. Taking $m_e = 0.27m_0$, we obtain $N(E) \approx 1 \cdot 10^{19} \text{cm}^{-3}$ for $E_c - E = 58$ meV. Assuming that all electrons in the conduction band come from the pump and taking into account that the penetration depth of UV pump photons is 100 nm and exciton life-time is ~ 100 ps, we estimate the necessary energy of the corresponding pulse to be of 1.4 μ J.

To clarify the nature of the 3rd component of the spectra, we calculated approximate dependences on the pump level of the possible upper (at T_1) and lower (at T_2) boundaries of the band gap E_g , as well as the corresponding differences $E_g - E_3$, where E_3 is the maximum energy of the 3rd component, using the approximate values of the lower (T_1) and upper (T_2) temperature limits (see Fig. 6). The results are presented in Fig. 7.

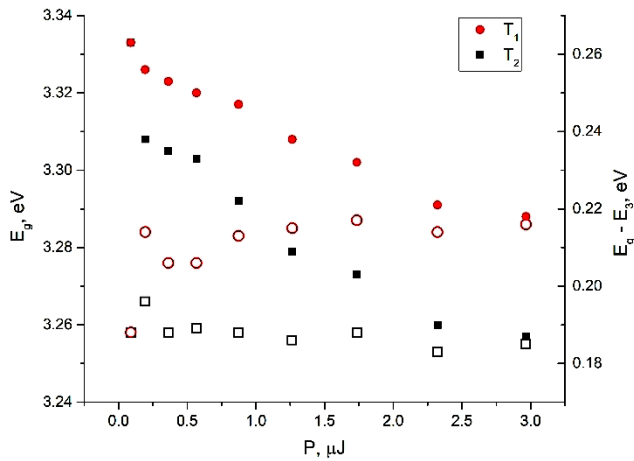


Fig. 7. Dependences on the pump level of the possible upper (at T_1) and lower (at T_2) boundaries of E_g and corresponding differences $E_g - E_3$, where E_3 is the maximum energy of the 3rd component (color online)

It is noteworthy that the values of $E_g - E_3$ shown in Fig. 7 are practically independent of pumping. This suggests that in the case under consideration the 3rd component of the spectra is due to radiation associated with the defect with energy level located at 0.19 – 0.21 eV below the bottom of the conduction band. Based on [27], it can be assumed that this defect is an interstitial Zn. Similar spectral band was observed in ZnO films grown on Si substrates [28]. It is quite possible that this band dominates at low pumping levels for the samples studied here and three-component decomposition is not completely correct in this case. This can cause an abrupt change in energy shifts in the pump range between 0.09 and 0.19 μJ in Fig. 5, where three-component decomposition was applied. It makes sense to note that during the pumping process, electrons from the valence band fall not only into the conduction band, but also to the defect level. And, since the lifetime of radiation from the level of the defect (usually of the order of microseconds) is significantly longer than the lifetime of the exciton, most of the electrons arriving during pumping can turn out to be at the level of defect. It is possible that this is one of the reasons for the absence of electron-hole plasma radiation that is possible at the pumping levels used.

We compare luminescence spectra for samples No. 1 and No. 2 in order to evaluate the role of Au. Fig. 9 shows spectra of two samples obtained at close pump levels of 1.8 μJ .

As can be seen in Fig. 8, the spectra of samples No. 1 and No. 2 are very similar to each other. The energy of the high-frequency component with increasing pumping remains almost constant, as in sample No. 1. Considering this component to be exciton radiation, we estimate the band-gap at room temperature. We obtain $E_g = 3.27 + 0.06 \approx 3.33$ eV, which practically does not differ from the value of E_g obtained for sample No. 1. The second component here, apparently, is the P line, and the third is the radiation due to the level of the defect. However, the shift in the energy of P line photons relative to the photon energy of the exciton component (Δ_{12}) in the sample with Au is somewhat larger, which probably indicates greater heating

of the sample by pumping because the heat capacity of gold is significantly lower than the heat capacity of oxide zinc. In general, Au shifts the spectrum toward the long-wavelength side as follows: the 1st component is shifted by 1-4 meV, the 2nd one is shifted by 10 - 11 meV and the 3rd one is shifted by 24 - 25 meV.

Since the distribution density of whiskers, i.e. radiating regions, for samples No. 1 and No. 2 is the same, an approximate comparison of the integrated intensities (A_i) of the components is possible. It turns out the following: Au increases the integrated intensity of the P-line (A_2) approximately 1.6 - 1.5 times, and the integrated intensity of the radiation due to the level of defect (A_3), approximately 1.3 times. In contrast to A_2 and A_3 , the integrated exciton radiation intensity (A_1) decreases slightly in the presence of Au. This is probably due to an increase in the number of inelastic collisions of excitons (A_2 increases) and, accordingly, there remains a smaller number of excitons that have not experienced collisions.

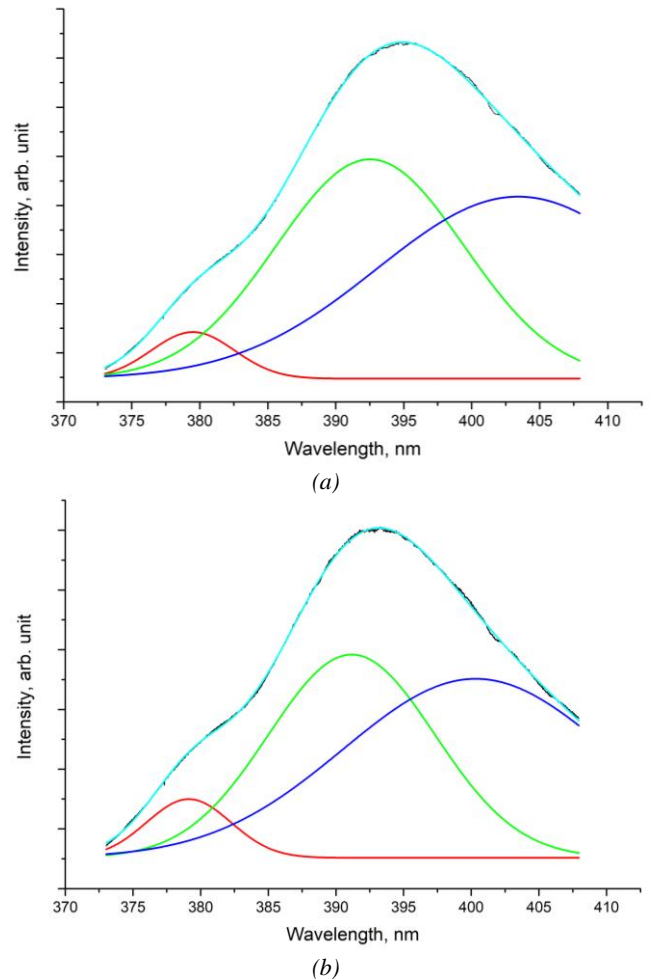


Fig. 8. Comparison of the spectra with Au (a) and without Au (b) at pump energy of $\sim 1.8 \mu\text{J}$ (color online)

The structure of the sample is very heterogeneous, therefore, the results obtained at different places on the surface may differ from each other. Particularly, there are places where not only spontaneous emission exists but also lasing appears with different values of the threshold pump

level. In Fig. 9 spectra obtained at one of these places are shown.

At a pump level below $0.7 \mu\text{J}$, only spontaneous luminescence occurs. Then several laser lines arise. With increasing pumping, these lines are preserved and new ones appear, which also remain with a further increase in pumping. It follows from this that lasing here does not occur according to the random lasing mechanism, when the radiation spectrum changes from pulse to pulse, but occurs in ZnO microcrystals, which play the role of micro resonators. The spectral region where the laser effect occurs is located in the region of the P line. There are places on sample's surface where lasing threshold is rather low ($\sim 0.1 - 0.15 \mu\text{J}$).

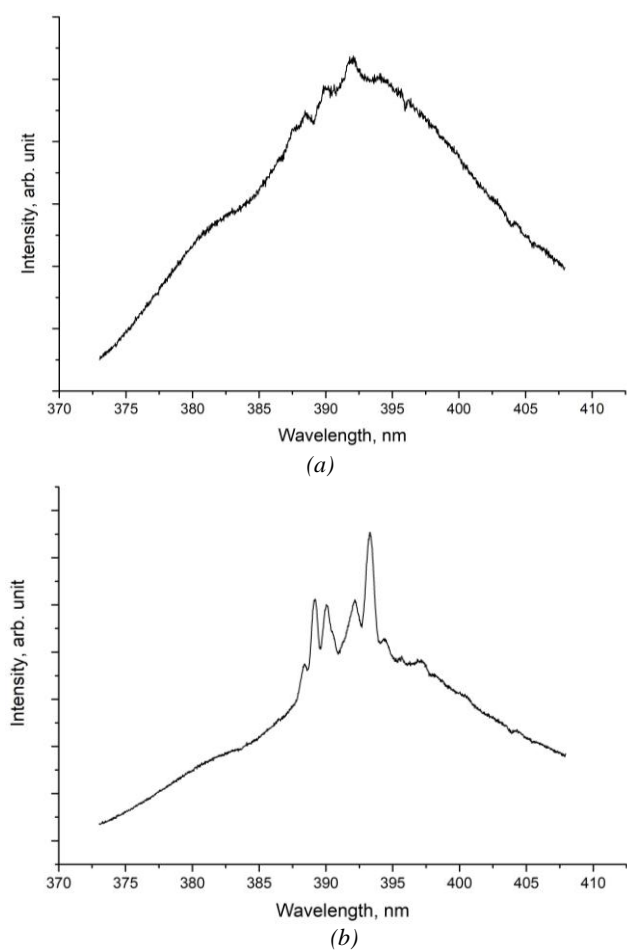


Fig. 9. PL spectra obtained at sample's area showing lasing: a) at pumping level of $0.75 \mu\text{J}$ (arising of lasing); b) at pumping level of $1.2 \mu\text{J}$ (lasing)

4. Conclusions

The edge emission of ZnO grown on whiskers was studied at room temperature with excitation by the 3rd harmonics of a pulsed Nd:YAG laser. The energy of the pump pulses was approximately from $0.1 \mu\text{J}$ to $3 \mu\text{J}$. Two variants of samples were considered: ZnO grown on whiskers without Au and ZnO grown on whiskers with Au. It was found that in all cases the spectrum consists of

three components. It was shown that the 1st (high-frequency) component is the exciton recombination radiation, the 2nd component is the P line, and the 3rd one is the radiation due to the level of the defect. The defect is most likely interstitial Zn.

It was shown that gold on whiskers significantly increases the intensity of P line and radiation due to the level of defect. In the sample with Au there are places where laser radiation occurs in the spectral region of the P line.

Acknowledgements

This work was supported by the Ministry of Education and Science of the Russian Federation within the State assignment for the Kotelnikov Institute of Radioengineering and Electronics of RAS "Spintronics" in part of the study of emission nature and within the State assignment for the FSRC "Crystallography and Photonics" RAS in part of film production and Russian Science Foundation (Project no. 18-29-12099 mk) in part of the study of the optical properties of the films. The use of the equipment of the Shared Research Center of the FSRS "Crystallography and Photonics" RAS was supported by the Ministry of Education and Science of the Russian Federation (project no. RFMEF162119X003).

References

- [1] D. M. Bagnall, Y. F. Chen, Z. Zhu, T. Yao, M. Y. Shen, T. Goto, *Appl. Phys. Lett.* **73**, 1038 (1998).
- [2] G. J. Lee, Y. Lee, H. H. Lim, M. Cha, S. S. Kim, H. Cheong, S. Min, S. H. Han, *J. Korean Phys. Soc.* **57**, 1624 (2010).
- [3] N. Ekthammathat, T. Thongtem, A. Phuruangrat, S. Thongtem, *J. Nanomater.* **2013**, 1 (2013).
- [4] C. M. Briskina, A. P. Tarasov, V. M. Markushev, M. A. Shiryaev, *J. Nanophotonics* **12**, 043506 (2018).
- [5] S. Rummyantsev, A. Tarasov, C. Briskina, M. Ryzhkov, V. Markushev, A. Lotin, *J. Nanophotonics* **10**(1), 016001 (2016).
- [6] M. Haupt, A. Ladenburger, R. Sauer, K. Thonke, R. Glass, W. Roos, J. P. Spatz, H. Rauscher, S. Riethmüller, M. Möller, *J. Appl. Phys.* **93**(10), 6252 (2003).
- [7] X. Hu, Y. Masuda, T. Ohji, K. Kato, *J. Am. Ceram. Soc.* **92**(4), 922 (2009).
- [8] N. Roy, A. Roy, *Ceram. Int.* **41**(3), 4154 (2015).
- [9] A. P. Tarasov, C. M. Briskina, V. M. Markushev, L. A. Zadorozhnaya, A. S. Lavrikov, V. M. Kanevskii, *JETP Lett.* **110**(11), 739 (2019).
- [10] P. Rauwel, M. Salumaa, A. Aasna, A. Galeckas, E. Rauwel, *J. Nanomater.* **2016**, 1 (2016).
- [11] T. V. Torchynska, B. El Filali, *J. Lumin.* **149**, 54 (2014).
- [12] Y. Lv, Z. Zhang, J. Yan, W. Zhao, C. Zhai, J. Liu, *J. Alloy. Compd.* **718**, 161 (2017).

- [13] M. M. Brewster, M. Y. Lu, S. K. Lim, M. J. Smith, X. Zhou, S. Gradecak, *J. Phys. Chem. Lett.* **2**(15), 1940 (2011).
- [14] A. P. Tarasov, C. M. Briskina, V. M. Markushev, L. A. Zadorozhnaya, I. S. Volchkov, *Opt. Mater.* **102**, 109823 (2020).
- [15] X. H. Xiao, F. Ren, X. D. Zhou, T. C. Peng, W. Wu, X. N. Peng, X. F. Yu, C. Z. Jiang, *Appl. Phys. Lett.* **97**, 071909 (2010).
- [16] L. Xu, S. Xiao, C. Zhang, G. Zheng, W. Rao, F. Xian, J. Miao, H. Wu, Z. Liu, *J. Optoelectron. Adv. M.* **16**(11), 1285 (2014).
- [17] H. Dong, S. Sun, L. Sun, W. Zhou, L. Zhou, X. Shen, Z. Chen, J. Wanga, L. Zhang, *J. Mater. Chem.* **22**, 3069 (2012).
- [18] A. S. Asvarov, A. K. Abduev, A. K. Akhmedov, V. M. Kanevsky, A. E. Muslimov, *Crystallogr. Rep.* **63**, 994 (2018).
- [19] J. Lu, C. Xu, J. Dai, J. Li, Y. Wang, Y. Lin, P. Li, *ACS Photonics* **2**, 73 (2015).
- [20] A. E. Muslimov, A. P. Tarasov, A. M. Ismailov, V. M. Kanevsky, *Tech. Phys. Lett.* **46**(12), 1223 (2020).
- [21] Y. Fang, Y. Wang, L. Gu, R. Lu, J. Sha, *Opt. Exp.* **21**, 3492 (2013).
- [22] A. Tarasov, V. Markushev, C. Briskina, S. Rummyantsev, A. Lotin, *J. Lumin.* **184**, 217 (2017).
- [23] A. M. Opolchentsev, L. A. Zadorozhnaya, Ch. M. Briskina, V. M. Markushev, A. P. Tarasov, A. E. Muslimov, V. M. Kanevskii, *Opt. Spectrosc.* **125**, 522 (2018).
- [24] E. I. Givargizov, *J. Vac. Sci. Technol. B* **11**(2), 449 (1993).
- [25] R. Matsuzaki, H. Soma, K. Fukuoka, K. Kodama, A. Asahara, T. Suemoto, Y. Adachi, T. Uchino, *Phys. Rev. B* **96**, 125306 (2017).
- [26] L. Wang, N. C. Giles, *J. Appl. Phys.* **94**(2), 973 (2003).
- [27] P. Erhart, K. Albe, A. Klein, *Phys. Rev. B* **73**, 205203 (2006).
- [28] M. V. Ryzhkov, V. M. Markushev, Ch. M. Briskina, S. I. Rummyantsev, A. P. Tarasov, *J. Appl. Spectrosc.* **81**(5), 877 (2014).

* Corresponding author: chara@cplire.ru